Title

Anti-mucin 4 fluorescent antibody brightly targets colon cancer in patient-derived orthotopic xenograft mouse models: A proof-of-concept study for future clinical applications

Journal

The American Journal of Surgery, 224(4)

ISSN

0002-9610

Authors

Turner, Michael A
Hollandsworth, Hannah M
Amirfakhri, Siamak
et al.

Publication Date

2022-10-01

DOI

10.1016/j.amjsurg.2022.05.036

Peer reviewed

HHS Public Access

Author manuscript

Am J Surg. Author manuscript; available in PMC 2023 March 06.

Published in final edited form as:

Am J Surg. 2022 October ; 224(4): 1081–1085. doi:10.1016/j.amjsurg.2022.05.036.

Anti-mucin 4 fluorescent antibody brightly targets colon cancer in patient-derived orthotopic xenograft mouse models: A proof-of-concept study for future clinical applications

Michael A. Turner[a,b], **Hannah M. Hollandsworth**[a,b], **Siamak Amirfakhri**[a,b], **Thinzar M. Lwin**[a,b], **Hiroto Nishino**[a,b], **Nicholas C. Neel**[a], **Gopalakrishnan Natarajan**[c], **Sukhwinder Kaur**[c], **Kavita Mallya**[c], **Robert M. Hoffman**[a,d], **Surinder K. Batra**[c], **Michael Bouvet**[a,b,*]

[a]Department of Surgery, University of California San Diego, 9300 Campus Point Dr, La Jolla, CA, 92037, USA

[b]VA San Diego Healthcare System, 3350 La Jolla Village Dr., San Diego, CA, 92161, USA

[c]Department of Biochemistry and Molecular Biology, University of Nebraska Medical Center, 985870 Nebraska Medical Center, Omaha, NE, 68198, USA

[d]AntiCancer, Inc., 7917 Ostrow St, San Diego, CA, 92111, USA

Abstract

Background: There is a high rate of positive surgical margins with resection of liver metastases in colorectal cancer (CRC). The present study reports using a fluorescent anti-mucin 4 (MUC4) antibodies to label primary CRC and liver metastases to better visualize tumor margins in mouse models.

Methods: Western blotting for MUC4 protein expression of normal colon and CRC tumor lysates was performed. Orthotopic primary and liver metastatic CRC mouse models received anti-MUC4 antibody conjugated to IR800 (MUC4-IR800). Mice were sacrificed and imaged after 48 hours.

Results: Western blotting demonstrated increased MUC4 expression in a human CRC cell line and patient-derived primary and liver-metastatic CRCs. The LS174T orthotopic primary CRC model tumor to background ratio (TBR) was 2.04 (±0.35). The patient-derived orthotopic xenograft (PDOX) primary CRC model TBR was 2.17 (±0.35). The PDOX liver metastasis model TBR was 1.56 (±0.53).

Conclusion: MUC4-IR800 provided bright labeling of primary and liver tumors in CRC orthotopic mouse models, demonstrating their future clinical potential for margin visualization in fluorescence guided surgery.

*Corresponding author. UCSD Moores Cancer Center, 3855 Health Sciences Drive #0987, La Jolla, CA, 92093-0987, USA. mbouvet@health.ucsd.edu (M. Bouvet).

Declaration of competing interest

RMH is a non-salaried affiliate of AntiCancer Inc. which uses PDOX models for contract research. All other authors have nothing to disclose.

1. Introduction

Resection remains the most effective treatment for colorectal cancer (CRC). However incomplete resection (i.e. positive surgical margins) is a poor prognostic indicator for CRC.[1] The liver is often the first site of metastasis for CRC and colorectal liver metastasis (CRLM), a recalcitrant disease and leading cause of death in CRC patients, develops in 50% of cases.[2] As in primary CRC, surgical resection remains the best treatment of CRLM for long term survival.[2] Positive margins on CRLM resection are associated with a decrease in overall survival.[3] The rate of R0 resection for CRLM is ~84–87%.[4,5]

Mucins, a family of epithelial glycoproteins, play an important role in forming a protective barrier between gut epithelium and the microbial milieu[6,7] as well as protecting against pH changes.[8] Their dysregulation has been implicated in the progression of colorectal cancer.[7] Mucin 4 (MUC4), expressed normally on the epithelial cell surface in the GI and respiratory tract, is over-expressed in several epithelial malignancies including CRC.[8,9] High expression of MUC4 has been associated with metastasis and as an independent indicator of worse prognosis in CRC.[6,7,9]

We have previously shown fluorescence guided surgery (FGS) is highly effective in CRLM resection with indocyanine green (ICG).[10] This previous study suggests using FGS with fluorescent antibodies may improve R0 resection rate for CRLM. This present study reports the use of a fluorescent antibody to MUC4 which brightly labels primary and liver metastasis CRC from patient derived as well as human cell line tumors.

2. Materials and methods

2.1 Animals

Female and male athymic nude mice (nu/nu) aged 4–6 weeks were purchased from the Jackson Laboratory (Bar Harbor, ME). Mice were maintained in a barrier room and fed an autoclaved laboratory approved diet. Prior to surgical procedures, mice were anesthetized with intraperitoneal injection of xylazine and ketamine cocktail reconstituted in phosphate-buffered saline (PBS). Post-procedure pain was treated with subcutaneous buprenorphine reconstituted in PBS. At the conclusion of the study, mice were euthanized with CO_2 inhalation, confirmed with cervical dislocation. All studies were approved by the San Diego Veterans Administration Medical Center Institutional Animal Care and Use Committee (IACUC, animal use protocol A17–020).

2.2 Antibody conjugation

Monoclonal MUC4 antibody (MUC4–8G7) was conjugated to IRDye800CW (LI-COR, Lincoln, NE) per manufacturer's protocol to establish MUC4-IR800. The dye was added to the antibody according to the dye manufacturer's protocol and incubated at room temperature on a shaker plate for 2 hours. Gel desalting columns (Thermo Fisher Scientific, Waltham, MA) were used for the purification process. After incubation, the antibody-dye combination was added to the gel desalting columns and centrifuged three times to remove unbound excess dye. The purified MUC4-IR800 antibody conjugate was then stored at 4 °C.

2.3 Western blotting

Lysates were obtained from normal colon, colon cancer cell line LS174T (ATCC, Manassas, VA) xenografts, and patient-derived colon cancer xenografts. The protein lysates were quantified using Bio-Rad protein assay reagents and standards. The total proteins (50 and 20 μg) were resolved in 2% sodium dodecyl sulfate (SDS) agarose gel for MUC4 because of its high molecular weight or 10% SDS-PAGE gel for GAPDH respectively. The resolved proteins were transferred onto a polyvinylidene difluoride (PVDF) membrane (Millipore; Billerica, MA, USA). The membranes were blocked for 1 hour with 5% non-fat dry milk diluted in phosphate buffered saline with tween 20 (PBST) at room temperature. The primary antibodies 8G7 for MUC4 or GAPDH were incubated with the membrane overnight at 4 °C. After three washes with PBST every 10 min, the membranes were incubated with respective horseradish peroxidase (HRP) conjugated secondary antibodies for 1 hour at room temperature. After incubation, membranes were washed with PBST three times, and signals visualized and developed using chemiluminescence reagent (Pierce ECL western blotting substrate, Ref #32106, Thermo scientific).

2.4 CRC orthotopic mouse model establishment

Human normal colon and patient-derived tumors were previously obtained under a University of California, San Diego-approved IRB protocol 140046 with written informed patient consent. The human colon cancer cell-line, LS174T (American Type Culture Collection, Manassas, VA), a patient-derived primary colon cancer (C4) and patient-derived liver metastasis colon cancer (Liver 2) were used for this study. To establish a LS174T cecal orthotopic model, previously grown subcutaneous LS174T tumors were grown in the cecum of nude mice using surgical orthotopic implantation.[11] This was accomplished by first sterilizing the anesthetized mouse's abdomen with 70% ethanol. Then a 1 cm incision was created on the lower abdomen, just left of midline.

Gentle pressure was then applied to deliver the cecum through the incision and the tumor fragment was sutured to the serosa of the lesser curve of the cecum with 8–0 nylon suture (Ethicon Inc., Somervile NJ). The cecum was then replaced to its anatomic position with care being taken to ensure the tumor fragment was not abutting the peritoneum. Peritoneum and skin were then closed with 6–0 nylon sutures (Ethicon Inc., Somerville, NJ). To establish a C4 cecal patient-derived orthotopic xenograft (PDOX) model, previously grown C4 subcutaneous tumors were used. The cecum was delivered through the mouse's abdomen as described above. 8–0 nylon suture (Ethicon Inc., Somervile NJ) was used to suture the tumor fragment to the cecum's serosa, and the cecum was returned to the body. To establish a Liver 2 liver implantation PDOX model, a 1.5 cm horizontal incision was made under the xyphoid of the anesthetized mouse. The liver was gently presented via this incision. Using a suture-less technique as described by Nishino et al.,[12] a small cavity was created in the liver bed, and the tumor fragment was placed there. Gentle pressure was applied to the liver until hemostasis was achieved. 6–0 nylon suture (Ethicon Inc., Somerville, NJ) was used to close the peritoneum and skin of all PDOX models. Tumors were allowed to grow for three weeks.[11,13,14]

2.5 Imaging

In vivo imaging was performed on the Pearl Trilogy Small Animal Imaging System (LI-COR Biosciences, Lincoln, NE) with wavelength excitement at 800 nm. MUC4-IR800 was administered via tail vein injection. A dose of 50 μg was chosen based on prior studies.[15,16] The LS174T subcutaneous model was administered MUC4-IR800 (50 μg) and imaged at 48 and 72 hours. The subcutaneous C4 and Liver 2 models were administered MUC4-IR800 (50 μg) and imaged at 24, 48, and 72 hours. The orthotopic models all received MUC4-IR800 (50 μg) and were euthanized 48 hours later. A laparotomy was performed to expose intra-abdominal organs. The mice were then imaged on the Pearl Trilogy Small Animal Imaging System (LI-COR Biosciences, Lincoln, NE). The Pearl Trilogy Small Animal Imaging System Software (LI-COR Biosciences, Lincoln, NE) was used to quantify the strength of the MUC4-IR800 signal. For the subcutaneous models, skin was used as background, and a tumor to background ratio (TBR) was derived by dividing the tumor signal by the background signal. For the LS174T and C4 primary tumor PDOX models, normal bowel was used as the background signal to calculate the TBR. For the Liver 2 liver PDOX model, the normal liver was used as the background signal to calculate the TBR.

2.6 Statistical analysis

Statistical descriptive analysis was performed using R software (Free Software Foundation, Boston, MA).

3. Results

Western blotting demonstrated mild expression of MUC4 in normal human colon lysates and no-expression in normal mouse colon lysates (Fig. 1). Varying levels of increased expression of MUC4 were demonstrated in human cancer cell line tumor tissue (LS174T) as well as patient derived primary colon cancer (C4) and patient derived liver metastasis colon cancer tissues (Liver 2) (Fig. 1).

All the subcutaneous CRC models demonstrated specific tumor labeling with MUC4-IR800 at 48 hours (data not shown). The mean TBR for the LS174T subcutaneous models (n = 2) was 2.09 (±0.06) and 2.62 (±0.11) at 48 and 72 hours, respectively. The mean TBR for the C4 subcutaneous models (n = 3) was 2.42 (±0.69) and 2.85 (±0.99) at 48 and 72 hours, respectively. The mean TBR for the Liver 2 subcutaneous model (n = 3) was 1.90 (±0.51) and 2.24 (±0.59) at 48 and 72 hours respectively.

The LS174T primary cancer orthotopic model (n = 2) had a mean TBR of 2.04 (±0.35) at 48 hours (Fig. 2). At 48 hours, the mean TBR for the primary C4 PDOX models (n = 3) was higher with a TBR of 2.17 (±0.35) (Fig. 3). Three Liver 2 PDOX models were established. However, 1 failed to grow a tumor and was therefore excluded from the analysis. For the remaining Liver 2 liver metastatic PDOX models (n = 2), the mean TBR was 1.56 (±0.53) at 48 hours (Fig. 4).

After in vivo imaging of the LS174T primary tumor orthotopic model, the tumor was resected and imaged on the LI-COR Odyssey to determine the depth of MUC4-IR800 penetration (Fig. 5). Imaging of a 1 cm diameter resected tumor demonstrated depth

of penetration of MUC4-IR800 throughout the tumor (Fig. 5a). Heat mapping imaging demonstrated the highest fluorescence signal intensity at the periphery of the tumor with moderate intensity throughout the rest of the tumor (Fig. 5b). The resected tumor was then processed for H&E staining of paraffin-embedded slides. H&E imaging on the Keyence FluorescenceMicroscope at 10x magnification confirmed the presence of LS174T CRC cells (Fig. 5c).

4. Discussion

We have previously shown FGS with ICG is effective in the resection of CRLM.[10] However, ICG is not tumor specific unlike the antibody-dye conjugate utilize in this present study. The previous study also addresses the potential of FGS to improve the resected tumor margins including the circumferential radial margin.[10] The present study demonstrated MUC4-IR800 provided distinct, specific, and bright labeling of colon cancer in cell line and PDOX primary tumor models. It also demonstrated MUC4-IR800 could successfully label a CRLM tumor in the liver bed with the Liver 2 PDOX liver metastasis model. This study serves as a proof of concept that intravenous administration of MUC4-IR800 leads to fluorescence visualization of colon cancer in orthotopic mouse models. Further studies that include imaging of additional PDOX models can confirm the use of MUC4-IR800 in a heterogeneous population of colon cancers, which can aid in translatability to clinical studies. Eventually large animal toxicity trials will need to be completed as a precursor to clinical trials.

Carcinomas are able to take advantage of MUC4's myriad functions to proliferate and avoid detection by the human immune system.[6,8] MUC4 has been implicated in the pathogenesis of pancreatic cancer[17] and dysregulation of MUC4 have been reported in several cancers including ovarian,[18] breast,[19] prostate,[20] gallbladder,[21] and biliary tract.[22] There are conflicting reports regarding MUC4 expression in CRC.[23] Dysregulation of several mucins, including MUC4, has been reported in CRC progression.[24] Ogata et al. examined mucin expression in surgical specimens and cancer cell lines, including LS174T which was used in the present study.[25] Myerscough et al. evaluated mucin expression in three tissue types, ulcerative colitis (UC), UC with dysplasia, and UC with carcinoma.[26] MUC4 expression was elevated in all 3 tissue types compared to normal colonic tissue, with the highest levels noted in UC with dysplasia and UC with carcinoma group. However, some studies reported decreased MUC4 in colonic dysplasia and cancer.[24] Shanmugam et al. reviewed 132 CRC patient samples from a single institution.[6] Normal colonic tissue had MUC4 staining in the lower 2/3rd of the normal crypt, but in CRC, MUC4 staining was strongest in the cytoplasm. In addition, most CRC cases had decreased MUC4 expression, although 25% of cases had increased expression. High-expressing MUC4 CRC cases were associated with significantly shorter disease-free survival times.

The field of FGS has grown in the last several years. We have recently published reviews of FGS including clinical studies using FGS.[27–29] Another review lists all the contrast agents currently undergoing FDA clinical trials.[30] The present study demonstrates fluorescently-label MUC4 antibody has clinical potential to improve R0 resection of CRC cancer, especially CRLM, which would be an important development in the field of FGS.

Limitations of the study include a small sample size which did not allow the authors to compare patient samples or cell lines and the use of immunocompromised mice. Another concern in fluorescence imaging is “off-labeling,” where the fluorescent-antibody conjugate binds to non- cancer tissue which normally expresses the molecular target (i.e. MUC 4). While signal was observed in the mouse bladder and liver to a lesser extent, there was still adequate distinct labeling of CRC tumors from normal surrounding tissue in all orthotopic models. Another limitation of using a mouse model is the inherit anatomical difference in liver size compared to humans. However the patient-derived orthotopic xenograft models have been shown to be more patient like[31] and a useful model for the development of tumor labeling for FGS.[27,29] Fluorescence labelling would also be a helpful guide for the superficial tumors on the liver, which is often the case with CRLM, and these liver tumors have been resected using indocyanine green and fluorescence guided surgery (FGS) in a clinical trial.[10]

In conclusion, MUC4-IR800 provides distinct and bright labeling of colon cancer cell-line and PDOX tumors in mouse models, including a liver metastasis PDOX model, with minimal background fluorescence. MUC4-IR800 also has potential for fluorescence guided surgery in colon cancer and malignant CRLM tumors.

Funding

This study was funded by VA Merit Review grant numbers 1 I01 BX003856-01A1 and 1 I01 BX004494-01 (MB) and NIH/NCI T32CA121938 (HH, MT).

Abbreviations:

FGS	Fluorescence guided surgery
CRC	Colorectal cancer
MUC4	Mucin 4
PDOX	Patient derived orthotopic xenograft
TBR	Tumor to background ratio
CRLM	Colorectal liver metastasis
ICG	Indocyanine green
PBS	Phosphate-buffered saline
SDS	sodium dodecyl sulfate
PBST	phosphate-buffered saline with tween 20
UC	Ulcerative colitis
HRP	horseradish peroxidase

References

1. Peeters KCMJ, Marijnen CAM Nagtegaal ID, et al. The TME trial after a median follow-up of 6 years: increased local control but no survival benefit in irradiated patients with resectable rectal carcinoma. Ann Surg. 2007;246(5):693–701. 10.1097/01.sla.0000257358.56863.ce. [PubMed: 17968156]
2. Mitchell D, Puckett Y, Nguyen QN. Literature review of current management of colorectal liver metastasis. Cureus. 11(1):e3940. doi:10.7759/cureus.3940. [PubMed: 30937238]
3. Garden OJ, Rees M, Poston GJ, et al. Guidelines for resection of colorectal cancer liver metastases. Gut. 2006;55(suppl 3). 10.1136/gut.2006.098053. iii1–iii8. [PubMed: 16835351]
4. Adam R, Kitano Y. Multidisciplinary approach of liver metastases from colorectal cancer. Ann Gastroenterol Surg. 2019;3(1):50–56. 10.1002/ags3.12227. [PubMed: 30697610]
5. Jonas S, Thelen A, Benckert C, et al. Extended resections of liver metastases from colorectal cancer. World J Surg. 2007;31(3):511–521. 10.1007/s00268-006-0140-3. [PubMed: 17308854]
6. Shanmugam C, Jhala NC, Katkoori VR, et al. Prognostic value of MUC4 expression in colorectal adenocarcinomas. Cancer. 2010;116(15):3577–3586. 10.1002/cncr.25095. [PubMed: 20564074]
7. Lu S, Catalano C, Huhn S, et al. Single nucleotide polymorphisms within MUC4 are associated with colorectal cancer survival. PLoS One. 2019;14(5), e0216666. 10.1371/journal.pone.0216666. [PubMed: 31091244]
8. Xia P, Choi AH, Deng Z, et al. Cell membrane-anchored MUC4 promotes tumorigenicity in epithelial carcinomas. Oncotarget. 2016;8(8):14147–14157. 10.18632/oncotarget.13122.
9. Jonckheere N, Skrypek N, Van Seuningen I. Mucins and pancreatic cancer. Cancers. 2010;2(4):1794–1812. 10.3390/cancers2041794. [PubMed: 24281201]
10. Tashiro Y, Aoki T, Hirai T, et al. Indocyanine green labeling of tumors in the liver recurring after radiofrequency ablation enables complete resection by fluorescence-guided surgery. Anticancer Res. 2022;42(3):1345–1350. 10.21873/anticanres.15603. [PubMed: 35220226]
11. Fu XY, Besterman JM, Monosov A, Hoffman RM. Models of human metastatic colon cancer in nude mice orthotopically constructed by using histologically intact patient specimens. Proc Natl Acad Sci Unit States Am. 1991;88(20):9345–9349. 10.1073/pnas.88.20.9345.
12. Nishino H, Hollandsworth HM, Sugisawa N, et al. Sutureless surgical orthotopic implantation technique of primary and metastatic cancer in the liver of mouse models. Vivo. 2020;34(6):3153–3157. 10.21873/invivo.12149.
13. Kuo TH, Kubota T, Watanabe M, et al. Liver colonization competence governs colon cancer metastasis. Proc Natl Acad Sci Unit States Am. 1995;92(26):12085–12089. 10.1073/pnas.92.26.12085.
14. Hoffman RM, ed. Patient-Derived Mouse Models of Cancer : Patient-Derived Orthotopic Xenografts (PDOX). Humana Press; 2017. 10.1007/978-3-319-57424-0.
15. Hollandsworth HM, Amirfakhri S, Filemoni F, et al. Anti-carcinoembryonic antigen-related cell adhesion molecule antibody for fluorescence visualization of primary colon cancer and metastases in patient-derived orthotopic xenograft mouse models. Oncotarget. 2020;11(4):429–439. 10.18632/oncotarget.27446. [PubMed: 32064046]
16. Hollandsworth HM, Amirfakhri S, Filemoni F, et al. Humanized anti-tumor-associated glycoprotein-72 for submillimeter near-infrared detection of colon cancer in metastatic mouse models. J Surg Res. 2020;252:16–21. 10.1016/j.jss.2020.02.017. [PubMed: 32217350]
17. Singh AP, Chaturvedi P, Batra SK. Emerging roles of MUC4 in cancer: a novel target for diagnosis and therapy: figure 1. Cancer Res. 2007;67(2):433–436. 10.1158/0008-5472.CAN-06-3114. [PubMed: 17234748]
18. Chauhan SC, Singh AP, Ruiz F, et al. Aberrant expression of MUC4 in ovarian carcinoma: diagnostic significance alone and in combination with MUC1 and MUC16 (CA125). Mod Pathol. 2006;19(10):1386–1394. 10.1038/modpathol.3800646. [PubMed: 16880776]
19. Mukhopadhyay P, Chakraborty S, Ponnusamy MP, Lakshmanan I, Jain M, Batra SK. Mucins in the pathogenesis of breast cancer: implications in diagnosis, prognosis and therapy. Biochim Biophys Acta. 2011;1815(2):224–240. 10.1016/j.bbcan.2011.01.001. [PubMed: 21277939]

20. Singh AP, Chauhan SC, Bafna S, et al. Aberrant expression of transmembrane mucins, MUC1 and MUC4, in human prostate carcinomas. Prostate. 2006;66(4): 421–429. 10.1002/pros.20372. [PubMed: 16302265]
21. Miyahara N, Shoda J, Ishige K, et al. MUC4 interacts with ErbB2 in human gallbladder carcinoma: potential pathobiological implications. Eur J Cancer Oxf Engl. 1990;44(7):1048–1056. 10.1016/j.ejca.2008.03.007, 2008.
22. Tamada S, Shibahara H, Higashi M, et al. MUC4 is a novel prognostic factor of extrahepatic bile duct carcinoma. Clin Cancer Res. 2006;12(14):4257–4264. 10.1158/1078-0432.CCR-05-2814. [PubMed: 16857800]
23. Das S, Rachagani S, Sheinin Y, et al. Mice deficient in Muc4 are resistant to experimental colitis and colitis-associated colorectal cancer. Oncogene. 2016;35(20): 2645–2654. 10.1038/onc.2015.327. [PubMed: 26364605]
24. Biemer-Hüttmann AE, Walsh MD, McGuckin MA, et al. Immunohistochemical staining patterns of MUC1, MUC2, MUC4, and MUC5AC mucins in hyperplastic polyps, serrated adenomas, and traditional adenomas of the colorectum. J Histochem Cytochem. 1999;47(8):1039–1048. 10.1177/002215549904700808. [PubMed: 10424888]
25. Ogata S, Uehara H, Chen A, Itzkowitz SH. Mucin gene expression in colonic tissues and cell lines. Cancer Res. 1992;52(21):5971–5978. [PubMed: 1394223]
26. Myerscough N, Warren B, Gough M, Corfield A. Expression of mucin genes in ulcerative colitis. Biochem Soc Trans. 1995;23(4). 10.1042/bst023536s, 536S–536S. [PubMed: 8654721]
27. Turner MA, Lwin TM, Amirfakhri S, et al. The use of fluorescent anti-CEA antibodies to label, resect and treat cancers: a review. Biomolecules. 2021;11(12):1819. 10.3390/biom11121819. [PubMed: 34944463]
28. Lwin TM, Hoffman RM, Bouvet M. The development of fluorescence guided surgery for pancreatic cancer: from bench to clinic. Expert Rev Anticancer Ther. 2018;18(7): 651–662. 10.1080/14737140.2018.1477593. [PubMed: 29768067]
29. Lwin TM, Turner MA, Amirfakhri S, Nishino H, Hoffman RM, Bouvet M. Fluorescence molecular targeting of colon cancer to visualize the invisible. Cells. 2022;11(2):249. 10.3390/cells11020249. [PubMed: 35053365]
30. Barth CW, Gibbs SL. Fluorescence image-guided surgery – a perspective on contrast agent development. Proc SPIE-Int Soc Opt Eng. 2020;11222:112220J. 10.1117/12.2545292.
31. Hoffman RM. Patient-derived orthotopic xenografts: better mimic of metastasis than subcutaneous xenografts. Nat Rev Cancer. 2015;15(8):451–452. 10.1038/nrc3972. [PubMed: 26422835]

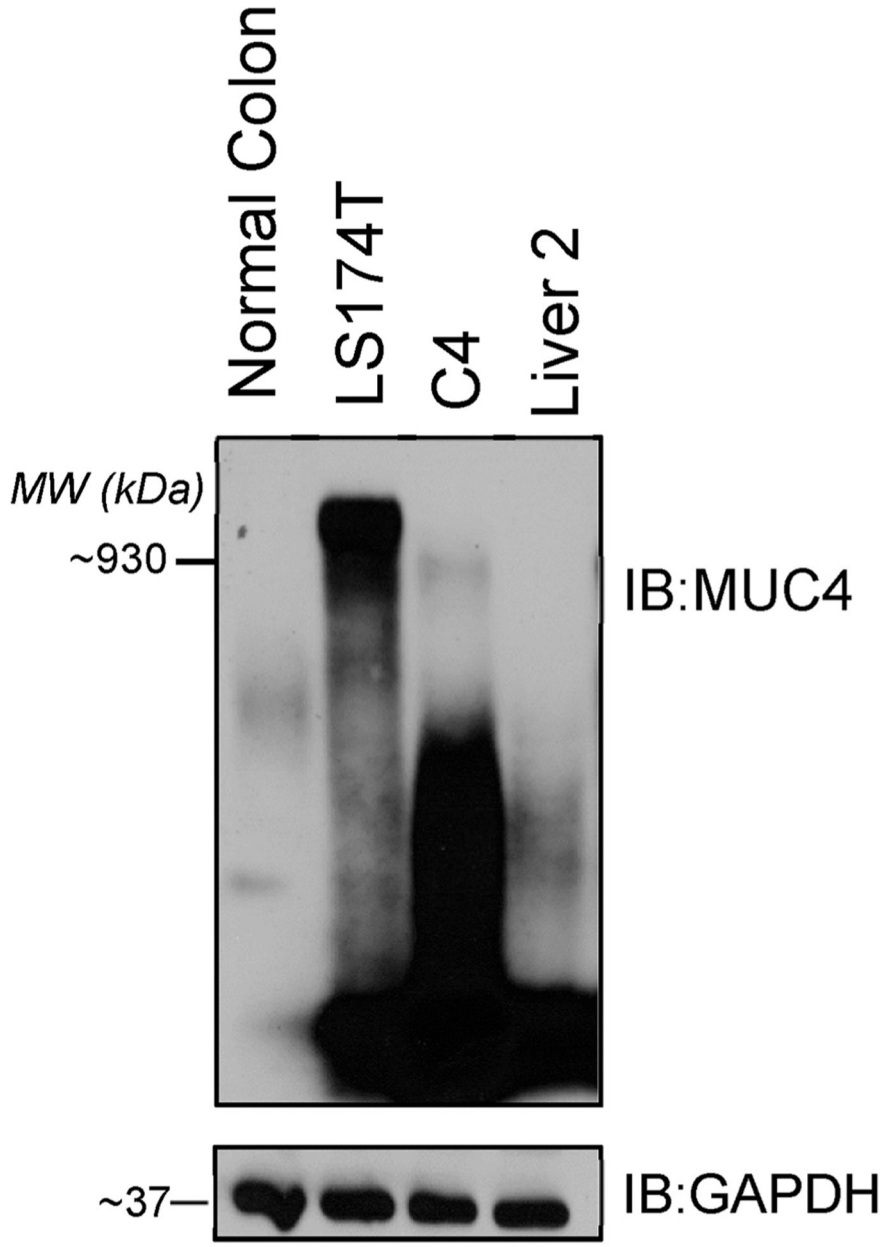

Fig. 1.

MUC4 Western blotting of normal human colon, human colon cancer cell line (LS174T), and cancer lysates of patient-derived primary tumors (C4) and patient-derived metastatic tumors (Liver 2).

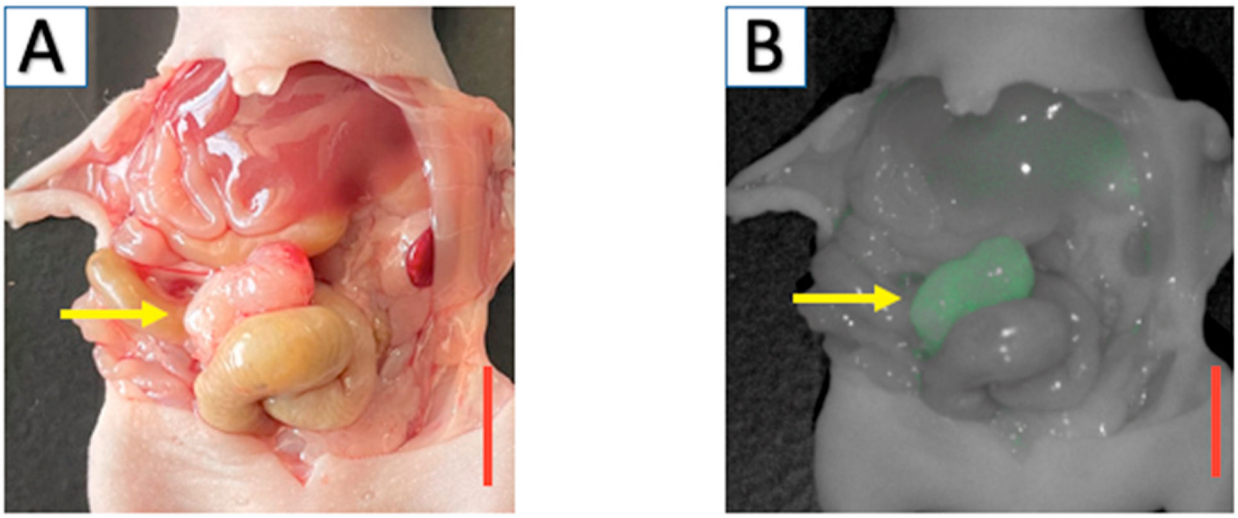

Fig. 2.

Orthotopic model of human cell line colon cancer tumor, LS174T, growing on the cecum (yellow arrow). (A) Bright light imaging demonstrating colonic tumor of approximately 6 mm in diameter (red bar represents 1 cm). (b) Fluorescence imaging after targeting with 50 μg of MUC4-IR800, 48 hours after administration.

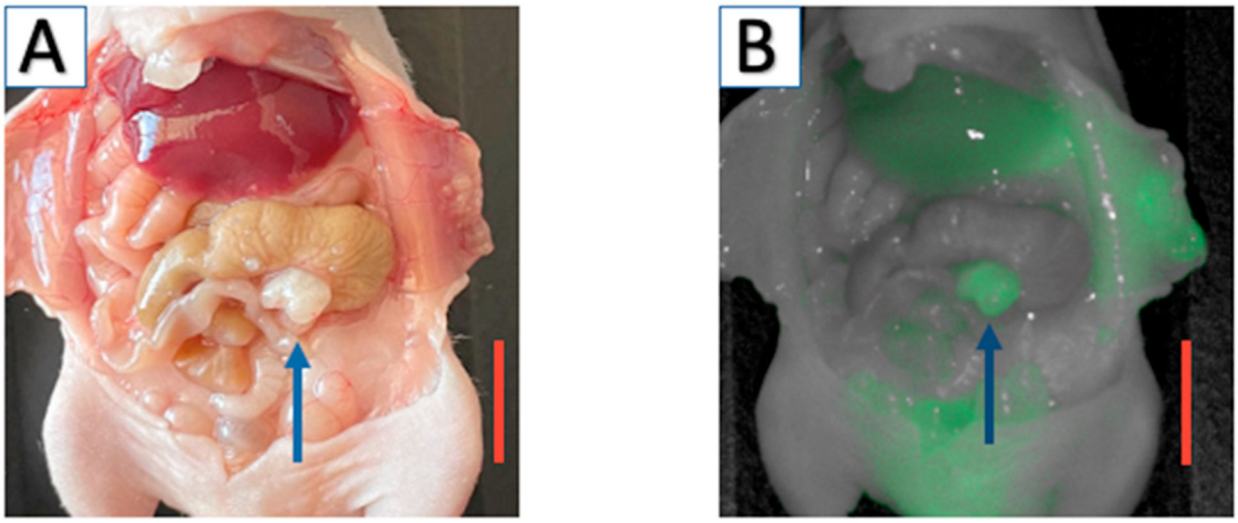

Fig. 3.

Orthotopic PDOX model of C4 patient-derived primary colon cancer growing on the cecum (blue arrow). (A) Bright light imaging demonstrating colonic tumor approximately 3 mm in diameter (red bar represents 1 cm). (b) Fluorescence imaging after targeting with 50 μg of MUC4-IR800, 48 hours after administration.

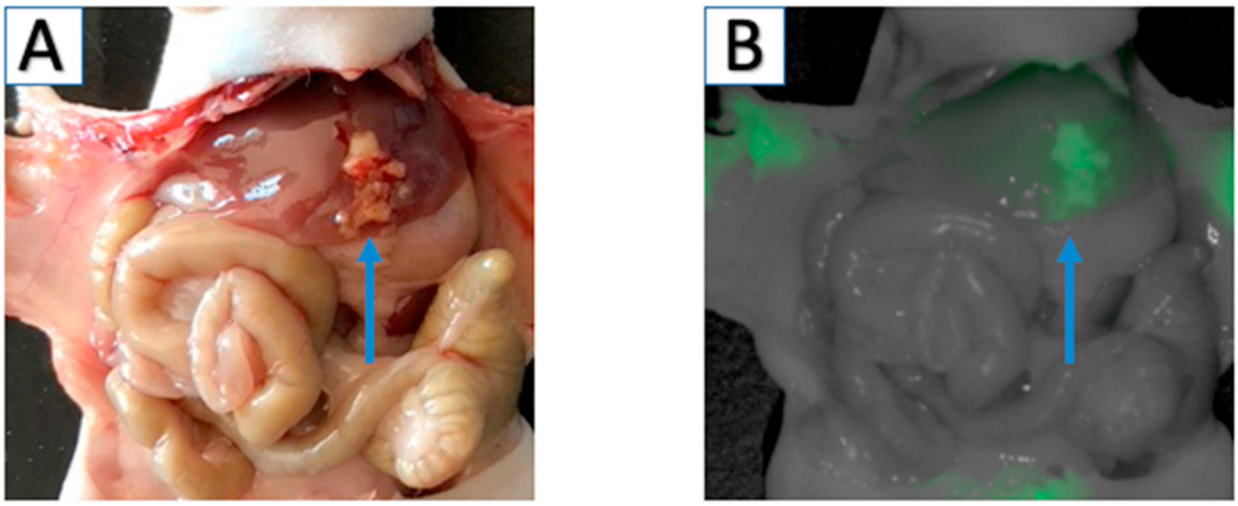

Fig. 4.

Orthotopic PDOX model of Liver 2 patient-derived colon cancer liver metastasis growing in the liver (blue arrow). (A) Bright light imaging demonstrating liver tumor. (b) Fluorescence imaging after targeting with 50 μg of MUC4-IR800, 48 hours after administration.

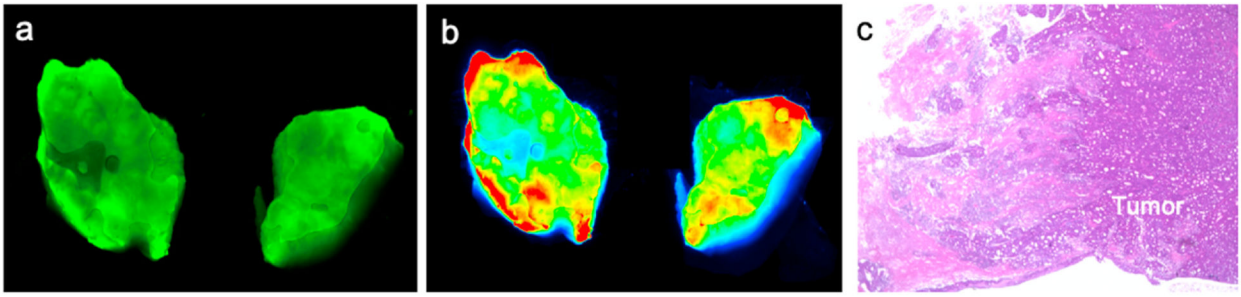

Fig. 5.

Cross-sectional imaging of LS174T tumor (1 cm) 48 h after administration of 50 μg of MUC4-IR800. (a) Fluorescence imaging on LI-COR Odyssey of the transected tumor demonstrated the depth of penetration throughout the tumor. (b) Heat map imaging of fluorescence demonstrating the highest fluorescence signal at the periphery of the tumor with moderate signal throughout. (c) H&E imaging confirms the presence of colon cancer cells histologically (10x magnification).